

# Similar chemical structures, dissimilar triplet quantum yields; CASPT2 model rationalizing the trend of triplet quantum yield in nitroaromatics systems.

Angelo Giussani<sup>\*,†,‡</sup> and Graham A. Worth<sup>†</sup>

<sup>†</sup>Department of Chemistry, University College London, 20 Gordon Street, London WC1H 0AJ, U.K.

<sup>\*</sup>To whom correspondence should be addressed. Email: Angelo.Giussani@uv.es

<sup>‡</sup>Current address: Instituto de Ciencia Molecular, Universitat de València, Apartado22085, ES-46071 Valencia, Spain

## Abstract

The photophysics of nitroaromatics compounds stand out for being characterized by an ultrafast decay into the triplet manifold and by a significant value of the triplet quantum yield. The latter quantity can change dramatically from one system to another, as proven for the molecules 2-nitronaphthalene, 1-nitronaphthalene, and 2methyl-1nitronaphthalene, whose triplet quantum yield have been previously measured to be  $0.93 \pm 0.15$ ,  $0.64 \pm 0.12$ , and  $0.33 \pm 0.05$ , respectively (J. Phys. Chem. A 2013, 117, 14100). In the present contribution we rationalize the reported trend for the triplet quantum yield on the basis of the different ability that the excited  $S_1$  state has in the three molecules to reach a non-previously characterized conical intersection with the ground state. Such a path is in competition with the one leading to triplet states population, which, on the basis of the present static description, appear to be equally favorable in the three systems. Performing high-level ab-initio computations, the energy barrier from the  $S_1$  CASPT2//CASSCF minimum to a CASPT2 minimum-energy-crossing-point of the mentioned  $S_1/S_0$  conical intersection have been computed to follow the same trend than the values of triplet quantum yield in the three nitroaromatics system here under analysis. The CASPT2 minimum-energy-crossing-point have been obtained using the projected constrained optimization method as recently implemented in the Molcas code. The same path has been characterized also for nitrobenzene, obtaining a value for the mentioned energy barrier that nicely fit in the model derived for the three nitro-naphthalene systems, and in agreement with its high value of the triplet quantum yield (greater than 0.8). The ability of the present model to not only rationalize the experimental data of a single molecule but to reproduce a trend for four slightly different systems speaks in favor of its reliability.

## Introduction

Nitroaromatic compounds (NCs) are an important class of molecules playing a prominent role in different fields among which: atmospheric pollution, energetic material, and in the drug delivery sector. Being formed as a result of incomplete combustion,<sup>1</sup> and having mutagenic and carcinogenic properties, NCs as 1-nitronaphthalene (1NN), 2-nitronaphthalene (2NN), and nitrofluorene constitute a considerable concern for urban air quality.<sup>2-5</sup> NCs and in particular nitrobenzene (NB) are common ingredients in energetic explosives, and NB-derived molecules are currently studied in order to obtain energetic compounds with better thermal stability.<sup>6</sup> Due to their photochemical properties, NB-derived molecules can be used as drugs able to photorelease with precise spatiotemporal resolution nitric oxide (NO),<sup>7</sup> which in turn is a key molecule having a variety of biological effects in the human body.

Beside their importance in the above mentioned fields, NCs usually display a rich photophysics and photochemistry, making of them fascinating systems in the study of molecule-light interactions. Regarding their photochemistry, most NCs photodegrade under UV excitation forming NO and the corresponding aryloxy radical,<sup>8-11</sup> although other photoproducts, as  $\text{NO}_2$  and O, can also be obtained.<sup>12</sup> More intriguingly is the fact that more than one single mechanism can be involved in the formation of the same photoproduct, as it is the case of NO photoproduction in NB where so-called roaming mechanisms can operate.<sup>13</sup> Regarding their photophysics, it is mainly characterized by a

rapid decay into the triplet manifold after light absorption. In particular 1NN is the organic compound with the fastest multiplicity change ever measured, decaying into the triplet state in around 100 fs.<sup>14-17</sup> The same time for triplet state population has also been claimed to characterize 2NN, although recent semiclassical non-adiabatic dynamics concluded that such a time scale is instead due to an  $S_2$ - $S_1$  internal conversion, while the intersystem crossing process leading to the triplet manifold should happen in around 0.7 ps.<sup>18</sup>

In order to understand the photophysics of NCs, a great deal of insights can be obtained by the study of a common property in a series of slightly different systems belonging to such a class of compounds. Such an approach was used by Vogt and Crespo-Hernández, who experimentally determined, among others properties, the triplet quantum yield for the three molecules 2NN, 1NN and 2-methyl-1-nitronaphthalene (2M1NN).<sup>19,20</sup> This series of molecules results particularly interesting, since despite their relative chemical similarity, the corresponding triplet quantum yield varies significantly:  $0.93 \pm 0.15$ ,  $0.64 \pm 0.12$ , and  $0.33 \pm 0.05$  for 2NN, 1NN, and 2M1NN, respectively. Performing DFT optimizations and vertical TD-DFT computations, Vogt and Crespo-Hernández obtained the following two results. First, in the ground state at larger torsion angles of the nitro group with respect to the plane of the naphthalene ring, a larger energy gap between the  $S_1$  and triplet states is observed. Second, the value of the torsion angle in the ground state minima increase along the series, being for example in acetonitrile equal to 0.3, 39.3, and 55.4 degrees for, 2NN, 1NN, and 2M1NN, respectively. These results made the authors conclude that the difference in the triplet quantum yield are related to the different torsion angles of the corresponding ground state minima, which in turn strongly influences the energy gap between singlet and triplet states, and then the probability of intersystem crossing.

In the present contribution the reason behind the experimentally recorded trend for the triplet quantum yield in the series 2NN, 1NN, and 2M1NN is reconsidered performing ab-initio CASPT2//CASSCF and CASPT2//CASPT2 computations. The work has been conducted at the light of the very low fluorescence emission recorded in the systems,<sup>21</sup> which consequently point out to the presence of an accessible non-radiative relaxation process, and of a recently characterized  $S_1/S_0$  conical intersection (CI) in the related molecule NB.<sup>22</sup> The obtained results shown that CIs displaying similar structural deformations are indeed present also for the three nitronaphthalene systems here under consideration, and that the different ability that the three molecules have to reach such a crossing point rather than a different ability to reach a singlet-triplet crossing region leading to the triplet states, constitutes a model able to rationalize the experimental trend of the triplet quantum yield along the 2NN, 1NN, and 2M1NN series (see Figure 1).

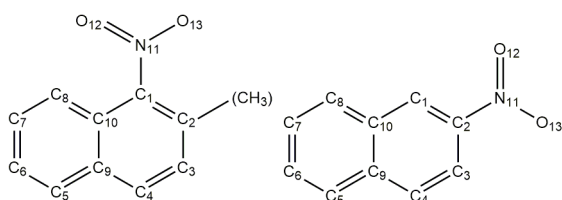


**Figure 1.** On the left, atom labeling for 1NN and 2M1NN; on the right, atom labeling for 2NN.

## METHODS

The present study has been performed employing the well-tested CASPT2 and CASSCF methods<sup>23-25</sup> as implemented in the OpenMolcas software.<sup>26</sup> Geometries optimizations have been performed either at the CASSCF level or at the CASPT2 level, in the latter case computing the required gradients numerically. In both cases, the final energies have been computed at the CASPT2 level, so to take into account the dynamic correlation effects. No restrictions to the symmetry of the molecule have been imposed ( $C_1$  symmetry). The basis set of atomic natural orbital (ANO) of L-type contracted to C,N [4s,3p,1d]/H[2s1p] has been employed.<sup>27,28</sup>

An active space composed of 18 active electrons distributed in 14 active orbitals has been used in all the final vertical calculations, and in both CASSCF and CASPT2 optimizations. As shown in

Figure S1 of the Supporting Information (SI), the selected active space takes into account both the  $\pi$  nature of the system and the lone pairs of the oxygen atoms.

Within the CASPT2 calculations, an imaginary level-shift correction of 0.2 au has been used to minimize the effects of possible intruder states. The CASPT2 standard zeroth-order Hamiltonian has been used as originally implemented.<sup>24</sup> The core orbitals have been frozen in the CASPT2 calculations. Such a CASPT2 approach has been validated in many different studies on organic molecules, providing a correct prediction, description, and interpretation of photophysical experimental data.<sup>25,29,30</sup>

In order to connect some important regions of the potential energy hypersurface (PEH), linear interpolation of internal coordinate (LIIC) calculations have been performed.<sup>31</sup> Minimum energy crossing points have been optimized using the projected constrained optimization method as recently implemented in Molcas.<sup>32</sup> The CI optimizations has been performed at the CASPT2 level, and not as CASPT2 vertical calculations performed along a CASSCF CI optimization.<sup>33</sup> In the regions of the potential energy hypersurfaces where two or more states of different spin multiplicity are degenerate, the corresponding SOC have been calculated, as described elsewhere.<sup>34</sup> The Cholesky decomposition has been used to speed up the calculation of two-electron integrals.<sup>35</sup>

## RESULTS AND DISCUSSION

The significant diversity in the value of the triplet quantum yield in the three molecules 2NN, 1NN, and 2M1NN (significantly decreasing along the series), reflects the different ability that the three systems have to decay into the triplet manifold. This in turn can be originated from either the fact that the decay path leading into the triplet manifold is less and less favorable in the series of molecules, and/or by the presence of a competing decay path not involving the population of the triplet states which becomes more and more favorable along the series of molecules. In order to evaluate the ability of the three systems to decay into the triplet manifold, the main decay path experimented by the excited  $S_1$  bright state has been characterized from the respective ground-state minima. The latter equilibrium geometries have been obtained at the CASPT2 level, since for the related system NB CASSCF-optimized ground state structures have been shown to display geometrical parameters that differ significantly with respect to the ones resulting from electron diffraction measurements, especially regarding the NO bond distances.<sup>22,36</sup> In the CASPT2 optimizations a CAS(18,14) active space has been employed, only the ground state root have been computed, and the corresponding CASPT2 gradients have been evaluated numerically using the OpenMolcas software. Due most probably to the use of just one root, the CAS(18,14) active space differ from the one later used for the computation of excited states by the presence of sigma orbitals instead that the full valence  $\pi$  space. The same effect was observed in a previous study on NB performed with a similar computational protocol.<sup>22</sup> In order to characterize the so obtained  $S_0$  minima, CASSCF(18,14) frequencies computations were performed, which have provided for all three cases no imaginary frequencies. CASPT2 frequencies computations have not been attempted due to the high computational cost required for the systems here under analysis, and for the limited precision that it is expected out of a numerical evaluation of them. We can however concluded, based on the obtained CASSCF(18,14) frequencies, that the CASPT2 ground-state minima are at least true CASSCF minima.

As shown in Figure 2, the three  $S_0$  minima display similar geometrical parameters, the only remarkable difference being the angle formed between the plane of the rings and the nitro group, as reflected by the values of the  $C_{10}C_1N_{11}O_{12}$  and  $C_2C_1N_{11}O_{12}$  ( $C_1C_2N_{11}O_{12}$  and  $C_3C_2N_{11}O_{12}$  for 2NN) dihedral angles. In qualitative agreement with previous DFT computations,<sup>19</sup> the ground state minimum is a planar geometry for the 2NN system, while for both 1NN and 2M1NN the nitro group is out of the rings-plane by around 45 and 70 degrees, respectively. Comparing the CASPT2(18,14) 1NN  $S_0$  minimum with a previously CASSCF(16,13) optimized structure<sup>37</sup> (see Figure S2), the most significant differences are seen in the values of the NO bond lengths, between 0.2-0.4 Å shorter at the CASSCF level.

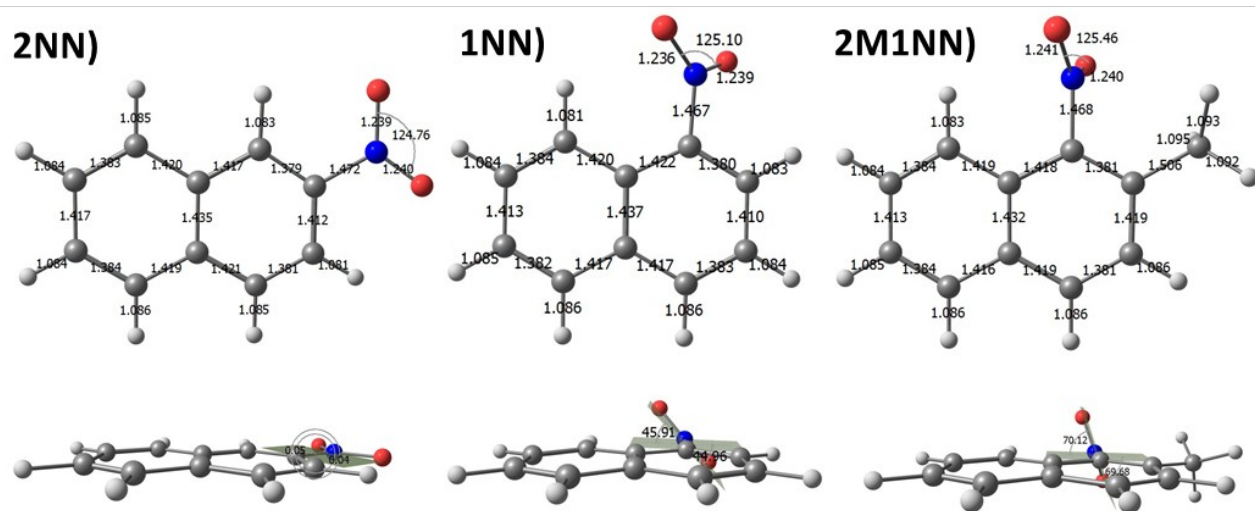


**Figure 2.** CASPT2(18,14) ground state minima of 2NN, 1NN, and 2M1NN. Selected bond lengths (in Å), angles, and dihedral angles (in degrees) are also reported.

The electronic structure of the obtained minima have been characterized computing the low-lying singlet and triplet excited states. In particular four singlet and five triplet excited states have been calculated, and the corresponding vertical energies, natures, and oscillator strengths are reported in Table 1. In all cases a very similar ordering of the states is observed, and the  $S_1$  ( ${}^1n_A\pi^*$ ) state appears nearly degenerated with the  $T_3$  ( ${}^3\pi_O\pi^*$ ) state. The latter two states are strongly coupled, as reflected by the corresponding SOC terms, equal to 75.71, 76.15, and 78.26  $\text{cm}^{-1}$  for 2NN, 1NN, and 2M1NN, respectively. The second lower  $S_2$  state, having  ${}^1(L_b\pi\pi^*)$  nature, is separated from the  $S_1$  ( ${}^1n_A\pi^*$ ) state in the three molecules by 0.20, 0.34, and 0.25 eV, respectively. In the recording of the triplet quantum yields, Vogt and Crespo-Hernández employed an excitation wavelength of 355 nm (3.49 eV), accordingly to which they claimed to initially populate the  $S_1$  state.<sup>19</sup> On the base of our results, it is concluded that at such experimental excitation the  $S_1$  ( ${}^1n_A\pi^*$ ) state is populated, being the only state below such an excitation energy apart from the  $S_2$  ( ${}^1(L_b\pi\pi^*)$ ) state in 2NN, which is however expected to decay in an ultrafast fashion into the  ${}^1(n_A\pi^*)$  state.<sup>18</sup> Performing TD-DFT computations Vogt and Crespo-Hernández instead concluded that the lowest and initially excited singlet state has  $\pi\pi^*$  nature. It must be noticed that their measurements were conducted in acetonitrile, and in their TDDFT computations such an environment was simulated using a PCM-like model. It can occur that in the used solved the ordering of the states differ with respect to the gas-phase, and that a  $\pi\pi^*$  instead that a  $n\pi^*$  state becomes the  $S_1$  root. Accordingly to our outcomes, the lowest  $\pi\pi^*$  state is the  ${}^1(L_b\pi\pi^*)$  state. On the basis of a simple analysis based on the value of the dipole moments (see Table S1) a inversion between the  ${}^1(L_b\pi\pi^*)$  and  ${}^1(n_A\pi^*)$  states when passing from the gas-phase to an acetonitrile solution is not predicted, being the two states characterized by similar values of the dipole moments. It must also be noticed that the  ${}^1(L_b\pi\pi^*)$  state has a much smaller coupling with the triplet manifold and in particular with the  ${}^3(\pi_O\pi^*)$  state, consequently making of the population of the triplet states an improbable process, which is in contrast with the significant triplet quantum yields recorded in the molecules. Finally, the reported  $S_1$  oscillator strengths in the paper of Vogt and Crespo-Hernández are much closer to the ones here characterizing the  ${}^1(L_b\pi\pi^*)$  state, making us suppose that such TDDFT computed state is the  ${}^1(L_b\pi\pi^*)$ , taking also into account the partial charge-transfer character of such a root,<sup>38</sup> the excited state energy underestimation of charge-transfer states in TDDFT,<sup>39</sup> and the general issue related with excited state ordering when computed with such a level of theory.<sup>40</sup> Another important point worth commenting is the zero oscillator strength characterizing the  ${}^1(n_A\pi^*)$  state at the here obtained 2NN ground state minimum. Being completely planar and consequently having  $C_s$  symmetry, the transition from the ground to the  ${}^1(n_A\pi^*)$  state results forbidden. The same

scenario is found in NB, whose ground state equilibrium structure is also totally planar.<sup>22</sup> In the latter system the population of the  $^1(n_A\pi^*)$  state is however possible due to low energy barrier along the torsional angle of the nitro group, which determines the coexistence of non-planar geometries from which  $^1(n_A\pi^*)$  promotions are allowed. In order to evaluate if such an explanation is also plausible for 2NN, the properties of a structure obtained from the  $^1(gs)_{\min}$  2NN through the torsion of the nitro group up to 45 degrees with respect to the plane of the naphthalene ring have been computed. At such a geometry the ground state energy has increased of only 0.03 eV with respect to the  $^1(gs)_{\min}$  2NN minimum, while the  $^1(n_A\pi^*)$  oscillator strength is now equal to 0.8963, for which it is possible to conclude that similarly to NB, the excitation of  $^1(n_A\pi^*)$  in 2NN can take places from accessible non-planar ground state structures.

**Table 1.** CASPT2(18,14) Vertical Excitation Energies at the Ground-State Minima ( $E_{VA}$ , eV) for the Lowest Valence Singlet and Spin Forbidden Triplet Excited States.<sup>a</sup>

2NN		1NN		2M1NN	
State	$E_{VA}(eV)$	State	$E_{VA}(eV)$	State	$E_{VA}(eV)$
$T_1^3(\pi\pi^*)$	2.66	$T_1^3(\pi\pi^*)$	2.53	$T_1^3(\pi\pi^*)$	2.63
$T_2^3(n_A\pi^*)$	3.09	$T_2^3(n_A\pi^*)$	3.10	$T_2^3(n_A\pi^*)$	3.12
$T_3^3(\pi_O\pi^*)$	3.23	$T_3^3(\pi_O\pi^*)$	3.32	$S_1^1(n_A\pi^*)$	3.33 (0.0013)
$S_1^1(n_A\pi^*)$	3.26 (0.0000)	$S_1^1(n_A\pi^*)$	3.36 (0.0041)	$T_3^3(\pi_O\pi^*)$	3.36
$T_4^3(\pi\pi^*)$	3.43	$T_4^3(\pi\pi^*)$	3.52	$T_4^3(\pi\pi^*)$	3.56
$S_2^1(L_b\pi\pi^*)$	3.46 (0.0069)	$S_2^1(L_b\pi\pi^*)$	3.70 (0.0021)	$S_2^1(L_b\pi\pi^*)$	3.61(0.0160)
$T_5^3(n_B\pi^*)$	3.70	$T_5^3(n_B\pi^*)$	3.73	$T_5^3(n_B\pi^*)$	3.72
$S_3^1(n_B\pi^*)$	3.79 ( $10^{-5}$ )	$S_3^1(n_B\pi^*)$	3.79 (0.0005)	$S_3^1(n_B\pi^*)$	3.89 ( $10^{-5}$ )
$S_4^1(L_a\pi\pi^*)$	4.30 (0.1764)	$S_4^1(L_a\pi\pi^*)$	4.05 (0.1057)	$S_4^1(L_a\pi\pi^*)$	4.12 (0.1159)

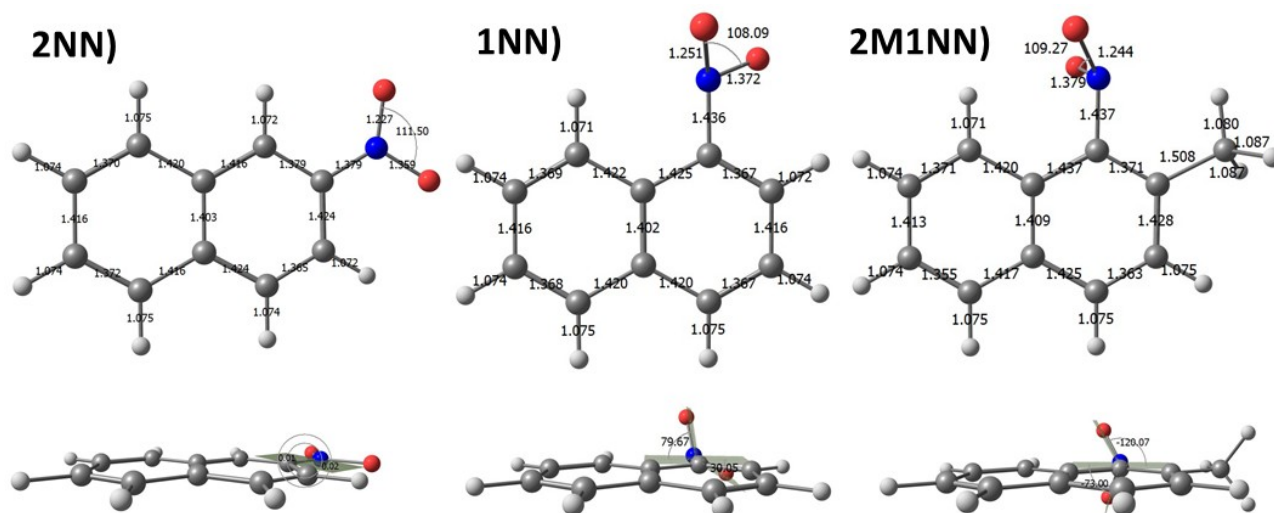
<sup>a</sup> The computed oscillator strengths for the singlet–singlet transitions are also and reported in parenthesis.

Being one of the main focuses of the present work the explanation of the recorded trend for the triplet quantum yield, and since the latter has been measured exciting the systems into the  $S_1$  state, after having characterized the excited states scenario at the Franck-Condon regions as above described, the following exploration has been obtained computing two singlet and two triplet states. The corresponding Frank-Condon energies are reported in Table 2. Comparing with the 5-roots results, a non despretiable blue shift in the  $^1(n_A\pi^*)$  state is observed, leading to the lost of degeneracy with the triplet  $^3(\pi_O\pi^*)$  state, whose energetic position appears to be less affected by the number of computed roots. From the three ground state minima, the relaxation experimented by the  $^1(n_A\pi^*)$  state has been evaluated computing the corresponding excited minima. The so-obtained equilibrium geometries, hereafter indicated as  $^1(n_A\pi^*)_{\min}$ , are shown in Figure 3, while the energies of the low-lying singlet and triplet states are reported in Table 2. To verify that true CASSCF minima have been obtained, the corresponding CASSCF frequencies have been calculated; no imaginary frequencies appeared, but for the 2NN  $^1(n_A\pi^*)_{\min}$  minimum, for which an imaginary value of  $i23.73\text{ cm}^{-1}$  has been calculated. The latter frequency mainly describes a pyramidalization of the nitrogen atom. In the three minima the  $^1(n_A\pi^*)$  state is almost degenerate in energy with the triplet  $^3(\pi_O\pi^*)$  state, and again a large SOC characterizes the two roots (67.36, 65.00, and 65.99  $\text{cm}^{-1}$  for 2NN, 1NN, and 2M1NN, respectively). Regarding the  $^1(n_A\pi^*)_{\min}$  geometries, the 2NN molecule appears completely planar, as in its ground state minimum, while both 1NN and 2M1NN are non-planar structures in which the nitro group displays a partial pyrimidalization.

**Table 2.** CASPT2(18,14) Energies (eV) for the Most Relevant Singlet and Triplet States at Different Critical Points.<sup>a</sup>

State Geometry	2NN				1NN				2M1NN			
	gs	<sup>1</sup> (n <sub>A</sub> π*)	<sup>3</sup> (π <sub>O</sub> π*)	<sup>3</sup> (n <sub>A</sub> π*)	gs	<sup>1</sup> (n <sub>A</sub> π*)	<sup>3</sup> (π <sub>O</sub> π*)	<sup>3</sup> (n <sub>A</sub> π*)	gs	<sup>1</sup> (n <sub>A</sub> π*)	<sup>3</sup> (π <sub>O</sub> π*)	<sup>3</sup> (n <sub>A</sub> π*)
<sup>1</sup> (gs) <sub>min</sub>	0.00	3.51	3.21	3.25	0.00	3.59	3.35	3.16	0.00	3.56	3.48	3.26
<sup>1</sup> (n <sub>A</sub> π*) <sub>min</sub>	0.78	2.86	3.04	2.84	1.63	3.04	3.09	3.14	1.48	3.05	3.10	3.13
( <sup>1</sup> n <sub>A</sub> π*/gs) <sub>CI</sub>	3.13	3.13	4.49	3.09	3.16	3.17	4.55	3.12	3.04	3.05	4.64	3.01

<sup>a</sup> All the reported values are referred to the corresponding ground state optimized geometry, <sup>1</sup>(gs)<sub>min</sub>.

**Figure 3.** CASPT2(18,14) <sup>1</sup>(n<sub>A</sub>π\*)<sub>min</sub> minima of 2NN, 1NN, and 2M1NN. Selected bond lengths (in Å), angles, and dihedral angles (in degrees) are also reported.

Based on the above presented outcomes, we can then conclude that the same static description is shared in the three molecules: the bright <sup>1</sup>(n<sub>A</sub>π\*)<sub>min</sub> is strongly coupled with the triplet <sup>3</sup>(π<sub>O</sub>π\*) state, as reflected by the reported high SOC values, and in its minimum the two roots are degenerated, which make of the corresponding intersystem crossing process a particularly favorable outcome. This scenario was already characterized for 1NN and used as a rationalization for the ultrafast singlet to triplet decay experimentally recorded in the molecule.<sup>41–43</sup> On the basis of the obtained static results, it is then presumable that after <sup>1</sup>(n<sub>A</sub>π\*) absorption, the path leading to triplet state population is equally favorable in the three molecules. This consequently point out to the presence of a competing path whose presence justify the loss in triplet quantum yield observed along the series. Such a consideration, together with the particularly low or even absent fluorescence emission in the three molecules, made plausible the presence of an accessible non-radiative decay path in competition with the singlet to triplet decay route. In our previous article on the related system NB, a non-radiative decay from the <sup>1</sup>(n<sub>A</sub>π\*) to the ground state was described, involving the presence of an accessible CI between the two states.<sup>22</sup> The latter geometry is characterized by a shortening of the CN bond, together with an enlargement of both NO distances, and a decrease in the ONO angles. In order to evaluate if such a path is also possible in the three nitronaphthalene systems, CASPT2 CI optimizations have been carried out using the projected constrained optimization method as recently implemented in the Molcas software, obtaining minimum energies crossing points (MECPs) between the <sup>1</sup>(n<sub>A</sub>π\*) and the ground state. MECPs are in general used as a model for the description of a CI seam, and in order to evaluate the relation between other critical point and the CI region.<sup>44</sup> Careful should however be taken in the use of such a model, based on the assumption that MECP are in a way the most representative point of a CI and from which internal

conversion phenomena are most likely to occur; in all CI points a population transfer can actually occur, and what is in general more important is the first encountered CI point rather than the MECP, as shown for example in the guanine photophysics.<sup>45</sup> In the present contribution we however decide to compute MECPs as a way of characterizing the CIs, since it will provide a strategy in order to compare the CI regions in the various molecules here studied. For each system here under study a MECP has been found, hereafter denoted as  $(^1n_A\pi^*/gs)_{CI}$ , which display indeed the same main geometrical deformations present in the related CI of NB (see Figure 3 and ref. 22).

The computed MECPs can be considered somehow along the same “deformation direction” characterizing the evolution of the systems from the ground state minima towards the  $(^1n_A\pi^*)$  equilibrium structures: in fact, at least for what concern the nitro group, the MECPs geometries display similar main deformations appearing also in the  $(^1n_A\pi^*)$  minima, which are, as it was the case in NB, a decrease in the CN distance and ONO angle, together with an enlargement of the NO bonds (see Figure 1-3, and Table S2).

Comparing the energies of the low-lying singlet and triplet states at the computed crossing point and ground-state and  $(^1n_A\pi^*)$  minima (see Table 2), the following observations can be drawn. First, each MECP is placed energetically below the corresponding  $(^1n_A\pi^*)$  vertical excitation energy at the ground state equilibrium structure, specifically 0.38, 0.42, and 0.51 eV below for 2NN, 1NN, and 2M1NN, respectively. This in turn means that after excitation, each of the three molecules has enough energy in order to reach the corresponding CI. Second, the energy difference between the  $(^1n_A\pi^*)$  minimum and the MECP is increasing along the series: 0.27 eV for 2NN, 0.13 eV for 1NN, and 0.00 eV for 2M1NN. The trend in the energy difference shows that the accessibility to the CI region is more and more favorable along the series of molecules, following an opposite trend that the experimental value of the triplet quantum yield.

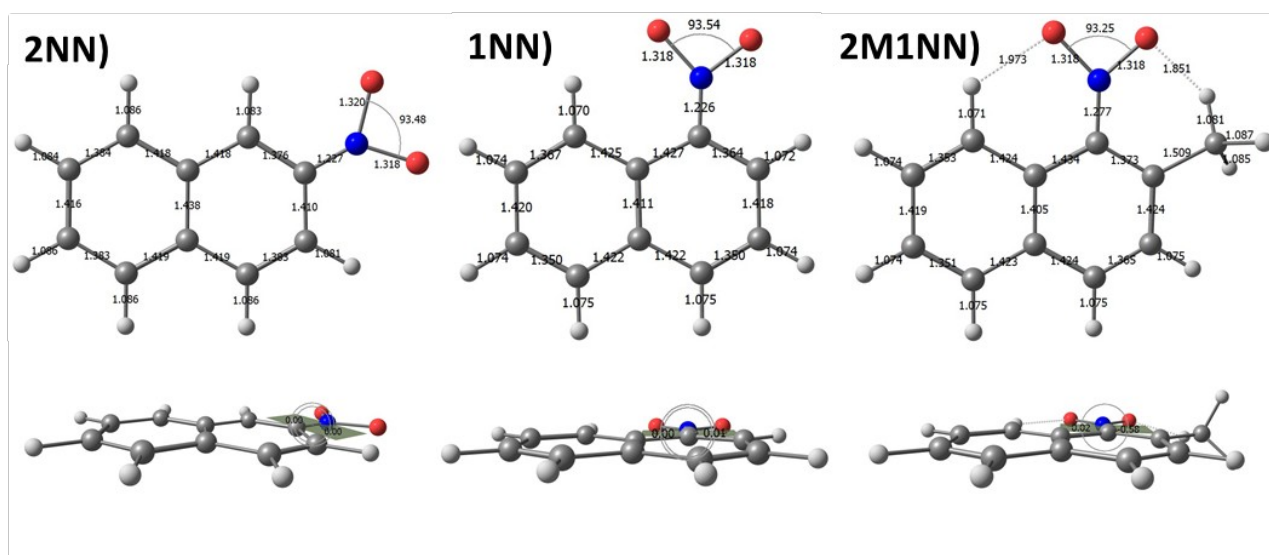


**Figure 4.** CASPT2(18,14)  $(^1n_A\pi^*/gs)_{CI}$  MECP of 2NN, 1NN, and 2M1NN. Selected bond lengths (in Å), angles, and dihedral angles (in degrees) are also reported.

In order to better characterize the potential energy hypersurfaces between the  $(^1n_A\pi^*)$  minima and the related MECP, LIIC computations between the two critical points have been performed, and the computed CASPT2(18,14) energies along them are presented in Table 3. As shown in Table 3, the  $(^1n_A\pi^*)$  energy initially decreases along the LIIC paths, despite the starting points were the  $(^1n_A\pi^*)$  minima. The behavior is probable imputable to the fact that the minima were obtained at the CASSCF(18,14) level, while the final energies are evaluated performing CASPT2(18,14) calculations. Evaluating the energy barrier as the difference between the lowest point along the LIIC path and the MECP, the next values are computed, again following the same trend as the one shown for the triplet quantum yields: 0.46, 0.42, and 0.19 eV for 2NN, 1NN, and 2M1NN, respectively.

Based on the presented results, we can formulate the following model that rationalize the trend for the values of the triplet quantum yield in the molecules 2NN, 1NN, and 2M1NN. After excitation into the  $S_1$   $^1(n_A\pi^*)$  state, the latter evolves in the three systems toward a minimum structure characterized by a strong coupling with the triplet  $^3(\pi_O\pi^*)$  state (large SOC and almost energy degeneration), which consequently constitutes a particularly favorable decay path leading into the triplet manifold. In the the three molecule a non-radiative decay path coexists along with the decay route into the triplet state, mediated by the presence of a CI between the  $^1(n_A\pi^*)$  and the ground state. While the decay path leading to triplet state population is equally favorable in the systems, the non-radiative repopulation of the ground state appear to be more and more favorable along the series of molecules, as reflected by the decreasing value of the energy barrier needed in order to reach the corresponding MECP from the related  $^1(n_A\pi^*)$  minimum. The importance that the non-radiative decay path acquires along the series made it competitive with the triplet route, consequently determining the lose of triplet quantum yield experimentally registered.

It can be argued that the computed energies barriers are not particularly high, also taking into account that they have been obtained out of LIIC paths, meanings that the above reported values constitute upper bounds of the true energies barriers. Such a fact, together with the favorable geometrical disposition of the excited minima and MECPs (i.e. being placed along the same deformation direction for the nitro group) point out that the described non-radiative decay should be relatively efficient. Nevertheless, most of the excited population but for 2M1NN, decay into the triplet manifold, indicating that despite the presence of an accessible non-radiative decay, the singlet-triplet coupling is strong enough as to make of the intersystem crossing process the most favorable relaxation route. It should be noticed that energy barriers of around 0.2 eV have been associated to excited state lifetimes of the order of the picosecond in DNA related systems;<sup>46</sup> considering that nitroaromatics systems can have ultrafast decay into the triplet manifold (as in 1NN, whose triplet states is populated in 100 fs after  $S_1$  absorption) it is then justifiable than the triplet route remain the main decay route in the nitroaromatics systems here studied.

In order to further validate the present static model, the latter has been applied also for the related system NB, in which the presence of a  $(^1n_A\pi^*/gs)_{CI}$  CI was originally described. From an optimized minimum energy crossing point obtained using the projected constrained optimization method starting from the NB CASPT2(14,11) CI, the corresponding LIIC path to between such a crossing region and the previously published CASSCF(14,11)  $^1(n_A\pi^*)$  minimum has been computed. A similar scenario has the one described for the nitronaphthalene systems has resulted, obtaining an energy difference between the minimum and the MECP of 0.36 eV, and an energy difference between the lowest LIIC point and the MECP of 0.48 eV (see Table 3). Performing picosecond time-resolved transient grating measurements in ethanol after excitation into the NB  $S_1$  state, Terazima and co-workers determined that the triplet quantum yield of NB is greater than 0.8.<sup>47,48</sup> Such quantities match with the proposed model: a 0.36 (0.48) eV barrier match with a triplet quantum yield greater that the one for 1NN and 2M1NN, having respectively a 0.13 (0.42) eV and 0.00 (0.19) eV energy barrier, and of the order of the triplet quantum yield characterizing the 2NN molecule, for which a barrier of 0.27 (0.46) eV have been obtained. Being NB the system for which the higher barrier has been computed, we would expect that the molecule displays the larger triplet quantum yield, a hypothesis that is plausible with the experimental determination of a value greater than 0.8.

It is interesting to notice that the two systems characterized by the higher energy gaps between the  $^1(n_A\pi^*)$  minimum and the corresponding MECP, i.e. NB and 2NN, are also the two systems displaying the smallest geometrical differences between such two critical points. In both molecules both the minima and the MECPs are totally planar, and the same main deformation are present. In the 1NN and 2M1NN molecules, the  $(^1n_A\pi^*/gs)_{CI}$  MECPs are again planar structures, but instead in the corresponding  $^1(n_A\pi^*)$  minima the nitro group is no longer coplanar with the naphthalene ring, and in both cases it has lost its own planar conformation displaying a certain degree of pyramidalization. Despite the larger geometrical deformations required in 1NN and 2M1NN than in

2NN and NB for evolving from the  $^1(n_A\pi^*)$  minimum to the  $(^1n_A\pi^*/gs)_{CI}$  MECP, the former systems are, as above reported, characterized by a lower energy barrier than the latter two molecules. As a final consideration, and since the present model is also based on the energy of the  $^1(n_A\pi^*)$  minimum, the 2NN CASSCF(18,14) equilibrium structure has been re-optimized starting from the previously described geometry obtained from the 2NN ground state minimum in which the nitro group has been placed at 45 degrees with respect to the plane of the rings. From such a geometry, characterized by a significant value of the oscillator strength for the electronic promotion into the  $^1(n_A\pi^*)$  state, the  $^1(n_A\pi^*)$  CASSCF(18,14) optimization has ended in the same region as described above, consequently validating the conclusion drawn from such a minimum.

**Table 3.** CASPT2(18,14) Computed Energies (eV) for the  $^1(n_A\pi^*)$  State Along the Computed LIIC Paths between  $^1(n_A\pi^*)_{min}$  Minima and  $(^1n_A\pi^*/gs)_{CI}$  MECPs.

Molecule	Geometry										
	$^1(n_A\pi^*)_{min}$	LIICg1	LIICg2	LIICg3	LIICg4	LIICg5	LIICg6	LIICg7	LIICg8	$(^1n_A\pi^*/gs)_{CI}$	$\Delta E^a$
2NN	<b>2.86</b>	2.79	2.73	2.69	<b>2.66</b>	2.67	2.70	2.79	2.93	<b>3.13</b>	0.47
1NN	<b>3.04</b>	2.96	2.96	2.83	2.78	<b>2.75</b>	2.75	2.89	3.03	<b>3.17</b>	0.42
2M1NN	<b>3.05</b>	3.01	2.91	2.91	2.90	2.88	<b>2.86</b>	2.86	3.00	<b>3.05</b>	0.19
NB	<b>2.85</b>	2.79	2.75	2.73	<b>2.72</b>	2.74	2.79	2.88	3.01	3.20	0.48

<sup>a</sup> Energy difference (eV) between the MECP and the lowest computed point along the LIIC.

## CONCLUSIONS

On the basis of high-level ab initio CASPT2//CASSCF and CASPT2 computations, a model rationalizing the experimental trend of the triplet quantum yield for the molecules 2NN, 1NN, and 2M1NN ( $0.93 \pm 0.15$ ,  $0.64 \pm 0.12$ , and  $0.33 \pm 0.05$ , respectively) after excitation into the  $S_1$  state has been proposed. The remarkable decrease in the triplet quantum yield observed along the series of molecules is here shown not to be caused by an increase in difficulty in reaching the singlet-triplet crossing region potentially leading to the triplet manifold, but to be attributable to an increase in the possibility to decay instead along a competitive non-radiative decay path mediated by an accessible non-previously reported conical intersection between the  $S_1$  and the ground-state.

The  $S_1$  state evolves in the three systems towards an equilibrium structure in which it is degenerate and strongly coupled with a triplet state, which can consequently be easily populated. This decay is common to the three molecules, for which we conclude that the path leading to the intersystem crossing process is equally favorable in all the here studied molecules.

From the  $S_1$  minimum, the systems can also further evolve towards the mentioned  $S_1/S_0$  conical intersection, and consequently decay non-radiatively. The probability to evolve along such non-radiative path appears to be system-dependent, as reflected by the computed energy barriers in the three systems in order to reach the conical intersection from the  $S_1$  minimum. The values of such barriers follow the same trend as the experimental values of the triplet quantum yields, larger for the systems characterized by a larger triplet quantum yield.

In order to compare the three CI regions in the three systems, minimum-energy crossing points for each CI have been obtained using the projected constrained optimization method as recently implemented in the OpenMolcas package.

The derived model has also been applied for the related system NB, and the results obtained match with the experimental value of the triplet quantum yield for the molecule.

The present contribution sheds light into the remarkable different photophysical behavior that the present molecules display, despite their similar chemical structures.

## AUTHOR INFORMATION

Corresponding Author

\*E-mail: angelo.giussani@uv.es.

### ORCID

Angelo Giussani: 0000-0002-9452-7641

### Notes

The authors declare no competing financial interest.

### ACKNOWLEDGMENTS

This project has received funding from the European Union's Horizon 2020 research and innovation programme under the Marie Skłodowska-Curie Grant Agreement No. 658173.

### REFERENCES

- (1) Handa, T.; Yamauchi, T.; Ohnishi, M.; Hisematsu, Y.; Ishii, T. Detection and Average Content Levels of Carcinogenic and Mutagenic Compounds from the Particulates on Diesel and Gasoline Engine Mufflers. *Environ. Int.* **1983**, *9*, 335.
- (2) Möller, L.; Lax, I.; Eriksson, L. C. Nitrated Polycyclic Aromatic Hydrocarbons: A Risk Assessment for the Urban Citizen. *Environ. Heal. Perspect.* **1993**, *101* (Environ. Heal. Perspect.), 309.
- (3) Xu, X.; Nachtman, J.; Rappaport, S.; Wei, E. Identification of 2 Nitrofluorene in Diesel Exhaust Particulates. *J. Appl. Toxicol.* **1981**, *1*, 196.
- (4) Wang, Y. I. Y.; Rappaport, S. M.; Sawyer, R. F.; Talcott, R. E.; Wei, E. T. Direct-Acting Mutagens in Automobile Exhaust. *Cancer Lett.* **1987**, *5*, 39.
- (5) Miller, J. A.; Sandin, R. B.; Miller, E. C.; Rush, H. P. The Carcinogenicity of Compounds Related to 2-Acetylaminofluorene. *Cancer Res.* **1955**, *15*, 188.
- (6) Sikder, A. K.; Maddala, G.; Agrawal, J. P.; Singh, H. Important Aspects of Behaviour of Organic Energetic Compounds: A Review. *J. Hazard. Mater.* **2001**, *84* (1), 1–26.
- (7) Nakagawa, H.; Hishikawa, K.; Eto, K.; Ieda, N.; Namikawa, T.; Kamada, K.; Suzuki, T.; Miyata, N.; Nabekura, J. I. Fine Spatiotemporal Control of Nitric Oxide Release by Infrared Pulse-Laser Irradiation of a Photolabile Donor. *ACS Chem. Biol.* **2013**, *8* (11), 2493–2500.
- (8) Chapman, O. L.; Heckert, D. C.; Reasoner, J. W.; Thackaberry, S. P. Photochemical Studies on 9-Nitroanthracene. *J. Am. Chem. Soc.* **1966**, *88* (23), 5550–5554.
- (9) Fukuhara, K.; Kurihara, M.; Miyata, N. Photochemical Generation of Nitric Oxide from 6-Nitrobenzo[a]Pyrene. *J. Am. Chem. Soc.* **2001**, *123* (36), 8662–8666.
- (10) Gerasimov, G. Y. Photochemical Degradation of Polycyclic Aromatic and Nitroaromatic Hydrocarbons in the Urban Atmosphere. *High Energy Chem.* **2004**, *38* (3), 161–166.
- (11) Phousongphouang, P. T.; Arey, J. Rate Constants for the Photolysis of the Nitronaphthalenes and Methylnitronaphthalenes. *J. Photochem. Photobiol. A Chem.* **2003**, *157* (2–3), 301–309.
- (12) Galloway, D. B.; Bartz, J. A.; Huey, L. G.; Crim, F. F. Pathways and Kinetic Energy Disposal in the Photodissociation of Nitrobenzene. *J. Chem. Phys.* **1993**, *98*, 2107.

- (13) Hause, M. L.; Herath, N.; Zhu, R.; Lin, M. C.; Suits, A. G. Roaming-Mediated Isomerization in the Photodissociation of Nitrobenzene. *Nat. Chem.* **2011**, *3*, 932.
- (14) Morales-cueto, R.; Esquivelzeta-rabell, M.; Saucedo-zugazagoitia, J.; Peon, J. Singlet Excited-State Dynamics of Nitropolycyclic Aromatic Hydrocarbons: Direct Measurements by Femtosecond Fluorescence Up-Conversion. **2007**, *111*, 552–557.
- (15) Zugazagoitia, S. J.; Almora-Díaz, C. X.; Peon, J. Ultrafast Intersystem Crossing in 1-Nitronaphthalene. An Experimental and Computational Study. *J. Phys. Chem. A* **2008**, *112*, 358.
- (16) Zugazagoitia, J. S.; Collado-fregoso, E.; Plaza-medina, E. F.; Peon, J. Relaxation in the Triplet Manifold of 1-Nitronaphthalene Observed by Transient Absorption Spectroscopy. **2009**, *113*, 805–810.
- (17) Vogt, R. A.; Reichardt, C.; Crespo-herna, C. E. Excited-State Dynamics in Nitro-Naphthalene Derivatives : Intersystem Crossing to the Triplet Manifold in Hundreds of Femtoseconds. *J. Phys. Chem. A* **2013**, *117*, 6580–6588.
- (18) Zobel, J. P.; Nogueira, J. J.; González, L. Mechanism of Ultrafast Intersystem Crossing in 2-Nitronaphthalene. *Chem. - A Eur. J.* **2018**, *24* (20), 5379–5387.
- (19) Vogt, R. A.; Crespo-Hernandez, C. E. Conformational Control in the Population of the Triplet State and Photoreactivity of Nitronaphthalene Derivatives. **2013**, *117*, 14100–14108.
- (20) Crespo-hernández, C. E.; R, A. V.; Sealey, B. Modern Chemistry & Applications On the Primary Reaction Pathways in the Photochemistry of Nitro-Polycyclic Aromatic Hydrocarbons. **2013**, *1* (3), 1–7.
- (21) Morales-cueto, R.; Esquivelzeta-rabell, M.; Saucedo-zugazagoitia, J.; Peon, J. Singlet Excited-State Dynamics of Nitropolycyclic Aromatic Hydrocarbons : Direct. *J. Phys. Chem. A* **2007**, 552–557.
- (22) Giussani, A.; Worth, G. A. Insights into the Complex Photophysics and Photochemistry of the Simplest Nitroaromatic Compound: A CASPT2//CASSCF Study on Nitrobenzene. *J. Chem. Theory Comput.* **2017**, *13* (6), 2777–2788.
- (23) Andersson, K.; Malmqvist, P.-A.; Roos, B. O. Second-Order Perturbation Theory with a Complete Active Space Self-Consistent Field Reference Function. *J. Chem. Phys.* **1992**, *96* (2), 1218.
- (24) Roos, B. O.; Andersson, K.; Fülcher, M. P.; Malmqvist, P.-Å.; Serrano-Andrés, L.; Pierloot, K.; Merchán, M. Multiconfigurational Perturbation Theory: Applications in Electronic Spectroscopy. *Adv. Chem. Phys.* **1996**, *93*, 219.
- (25) Serrano-Andrés, L.; Merchán, M.; Schleyer, P. v. R.; Schreiner, P. R.; Schaefer, H. F.; Jorgensen, W. L.; Thiel, W.; Glen, R. C. *Encyclopedia of Computational Chemistry*; 2004.
- (26) Aquilante, F.; Autschbach, J.; Carlson, R.; Chibotaru, L.; Delcey, M. G.; De Vico, L.; Fernández Galvan, I.; Ferré, N.; Frutos, L. M.; Gagliardi, L.; et al. MOLCAS 8: New

Capabilities for Multiconfigurational Quantum Chemical Calculations across the Periodic Table. *J. Comput. Chem.* **2016**, *37*, 506.

- (27) Widmark, P.-O.; Malmqvist, P.-Å.; Roos, B. O. Density Matrix Averaged Atomic Natural Orbital (ANO) Basis Sets for Correlated Molecular Wave Functions. *Theor. Chem. Acc.* **1990**, *77*, 291.
- (28) Pierloot, K.; Dumez, B.; Widmark, P.-O.; Roos, B. O. Density Matrix Averaged Atomic Natural Orbital (ANO) Basis Sets for Correlated Molecular Wave Functions. *Theor. Chim. Acta* **1995**, *90*, 87.
- (29) Merchán, M.; Serrano-Andrés, L.; Olivucci, M. *Computational Photochemistry*, 1st ed.; Olivucci, M., Ed.; Elsevier: Amsterdam, 2005; Vol. 16.
- (30) Giussani, A.; Pou-Amérigo, R.; Serrano-Andrés, L.; Freire-Corbacho, A.; Martínez-García, C.; Fernández P, M. I.; Sarakha, M.; Canle L, M.; Santaballa, J. A. Combined Theoretical and Experimental Study of the Photophysics of Asulam. *J. Phys. Chem. A* **2013**, *117* (10), 2125–2137.
- (31) Giussani, A.; Serrano-Andrés, L.; Merchán, M.; Roca-Sanjuán, D.; Garavelli, M. Photoinduced Formation Mechanism of the Thymine–Thymine (6–4) Adduct. *J. Phys. Chem. B* **2013**, *117*, 1999.
- (32) Galván, I. F.; Delcey, M. G.; Pedersen, T. B.; Aquilante, F.; Lindh, R. Analytical State-Average Complete-Active-Space Self-Consistent Field Nonadiabatic Coupling Vectors: Implementation with Density-Fitted Two-Electron Integrals and Application to Conical Intersections. *J. Chem. Theory Comput.* **2016**, *12* (8), 3636–3653.
- (33) Borin, A. C.; Giussani, A. Relaxation Mechanisms of 5-Methylcytosine.
- (34) Merchán, M.; Serrano-Andrés, L.; Robb, M. A.; Blancafort, L. Triplet-State Formation along the Ultrafast Decay of Excited Singlet Cytosine. *J. Am. Chem. Soc.* **2005**, *127*, 1820.
- (35) Pedersen, T. B.; Lindh, R.; Aquilante, F. Density Fitting with Auxiliary Basis Sets from Cholesky Decompositions. *Theor. Chem. Acc.* **2009**, *124*, 1.
- (36) Domenicano, A.; Schultz, G.; Hargittai, I.; Colapietro, M.; Portalone, G.; George, P.; Bock, C. W. Molecular Structure of Nitrobenzene in the Planar and Orthogonal Conformations - A Concerted Study by Electron Diffraction, X-Ray Crystallography, and Molecular Orbital Calculations. *Struct. Chem.* **1990**, *1* (1), 107–122.
- (37) Giussani, A. Toward the Understanding of the Photophysics and Photochemistry of 1 - Nitronaphthalene under Solar Radiation: The First Theoretical Evidence of a Photodegradation Intramolecular Rearrangement Mechanism Involving the Triplet States. **2014**.
- (38) Zobel, J. P.; Nogueira, J. J.; González, L. Quenching of Charge Transfer in Nitrobenzene Induced by Vibrational Motion. *J. Phys. Chem. Lett.* **2015**, *6*, 3006.

- (39) Dreuw, A.; Weisman, J. L.; Head-Gordon, M. Long-Range Charge-Transfer Excited States in Time-Dependent Density Functional Theory Require Non-Local Exchange. *J. Chem. Phys.* **2003**, *119* (6), 2943–2946.
- (40) Arulmozhiraja, S.; Coote, M. L. L a and 1 L b States of Indole and Azaindole : Is Density Functional Theory Inadequate ? **2012**, 575–584.
- (41) Orozco-Gonzalez, Y.; Coutinho, K.; Peon, J.; Canuto, S. Theoretical Study of the Absorption and Nonradiative Deactivation of 1-Nitronaphthalene in the Low-Lying Singlet and Triplet Excited States Including Methanol and Ethanol Solvent Effects. *J. Chem. Phys.* **2012**, *137*, 54307.
- (42) Giussani, A. Toward the Understanding of the Photophysics and Photochemistry of 1-Nitronaphthalene under Solar Radiation: The First Theoretical Evidence of a Photodegradation Intramolecular Rearrangement Mechanism Involving the Triplet States. *J. Chem. Theory Comput.* **2014**, *10* (9), 3987–3995.
- (43) Yang, M.; Zhang, T.; Xue, J.; Zheng, X. Ab Initio Study of Decay Dynamics of 1-Nitronaphthalene Initiated from the S<sub>2</sub>(Ππ\* + NNOπ) State. *J. Phys. Chem. A* **2018**, *122* (10), 2732–2738.
- (44) Serrano-pérez, L. S. J. *J. Handbook of Computational Chemistry*; 2012.
- (45) Serrano-Andrés, L.; Merchán, M.; Borin, A. C. A Three-State Model for the Photophysics of Guanine. *J. Am. Chem. Soc.* **2008**, *130* (8), 2473–2484.
- (46) Li, Q.; Giussani, A.; Segarra-Martí, J.; Nenov, A.; Rivalta, I.; Voityuk, A. A.; Mukamel, S.; Roca-Sanjuán, D.; Garavelli, M.; Blancafort, L. Multiple Decay Mechanisms and 2D-UV Spectroscopic Fingerprints of Singlet Excited Solvated Adenine-Uracil Monophosphate. *Chem. - Eur. J.* **2016**, *22*, 7497.
- (47) Takezaki, M.; Hirota, N.; Terazima, M. Nonradiative Relaxation Processes and Electronically Excited States of Nitrobenzene Studied by Picosecond Time-Resolved Transient Grating Method. *J. Phys. Chem. A* **1997**, *101*, 3443.
- (48) Takezaki, M.; Hirota, N.; Terazima, M. Relaxation of Nitrobenzene from the Excited Singlet State. *J. Chem. Phys.* **1998**, *108*, 4685.